Trans. JSASS Aerospace Tech. Japan
Vol. 10, No. ists28, pp. Pe_65-Pe_71, 2012

***Original Paper***

# Post-Test Sample Analysis of a Low Density Ablator Using Arcjet

By Takeharu SAKAI[1)], Keiichi OKUYAMA[2)], Yusuke KOBAYASHI[1)], Masami TOMITA[1)], Toshiyuki SUZUKI[3)], Kazuhisa FUJITA[3)], Sumio KATO[4)] and Seiji NISHIO[5)]

[1)]*Department of Aerospace Engineering, Nagoya University, Nagoya, Japan*
[2)]*Graduate school of Engineering, Aichi University of Technology, Gamagori, Japan*
[3)]*Japan Aerospace Exploration Agency, Tokyo, Japan*
[4)] *Department of Mechanical Systems Engineering, University of The Ryukyus, Nishihara, Japan*
[5)] *Kawasaki Heavy Industries, Kagamigahara, Japan*

(Received June 27th, 2011)

An existing computer code named super charring materials ablation (SCMA) is updated by implementing a coking process, in which a pyrolysis gas cokes within a char layer. The conservation equations for masses for resin, and coke, and energy are given. A coking rate equation is calculated by accounting for mass conservation of carbon deposited within a char layer. The method so upgraded is applied to the post-test sample analysis of the in-depth density profile for a low density ablator heated in an arcjet wind tunnel under one operating condition to evaluate the temperature variation of mass fraction of carbon contained in a pyrolysis gas used in the coking rate equation. The calculated result between with and without coking is compared to discuss the effect of coking on ablation behaviors.

**Key Words:** Ablation, Carbon-Phenolic Ablator, Coking, Numerical Simulation

**Nomenclature**

| | | |
|---|---|---|
| $c_p$ | : | specific heat at constant pressure |
| $e$ | : | internal energy |
| $h$ | : | enthalpy |
| $\dot{m}$ | : | flow rate |
| $p$ | : | pressure |
| $q$ | : | cold wall heating rate |
| $R$ | : | rate of pyrolysis or coking |
| $T$ | : | translational-rotational temperature |
| $\Delta x$ | : | thickness of an ablator |
| $\kappa$ | : | thermal conductivity |
| $\rho$ | : | density |
| $\omega_c$ | : | carbon mass fraction |

Subscripts

| | | |
|---|---|---|
| $c$ | : | char residual or carbon |
| *coke* | : | deposited carbon |
| *st* | : | stagnation (pitot) pressure |
| *pyro* | : | decomposition of resin |
| $g$ | : | pyrolysis gas |
| $r$ | : | resin |
| $v$ | : | virgin |

## 1. Introduction

When a space vehicle enters into the atmosphere of a planet with a very high speed, the space vehicle will be exposed to a significant aerodynamic heating. A carbon-phenolic ablator is often used to protect the space vehicle from such an aerodynamic heating. Recently, a low density carbon-phenolic ablator named Lightweight Ablator series for Transfer vehicle (called LATS, hereafter) has been developed by Okuyama of Aichi University of Technology. The specific gravity of LATS is from 0.3 to 0.7, which is lower by up to about one-fifth when compared with that of a typical carbon-phenolic ablator used in the past space missions. Such a low density ablator will be a promising material for an ablative thermal protection system of a space vehicle in future missions in Japan.

Qualitative ablative behaviors in a carbon phenolic ablator during heating are relatively well known. When the ablator is heated, the virgin material decomposes thermally to a mixture of gas containing hydrogen or hydrocarbon species etc, and a solid carbon residue. The thermally decomposed gas is called pyrolysis gas and the layer of the solid residue is called char. During heating, the pyrolysis layer deepens into the virgin material continuously, forming a layer made mostly by char and carbon fiber. We may call it char layer, hereafter. The pyrolysis gas diffuses within a char layer and escapes from the surface, resulting in the reduction of heating rate transferred into the ablator. Such a physical process should be predicted quantitatively from a thermal protection point of view.

The mechanisms of the char formation during ablation in a low density carbon-phenolic ablator are not well known. In particular, a coking process in the char layer is unknown. Coking is considered as a phenomenon that a solid carbon is deposited when a pyrolysis gas passes through a porous char layer to a surface.[1)] Although detailed physical and chemical conditions for coking are generally unknown, the coking phenomenon can be confirmed by a material density increase in the char layer toward the surface of a heated material. [1)] We confirmed such a trend in the in-depth density profile when the post-test sample of LATS heated in an arcjet wind tunnel is analyzed in our recent study[2)]. It is unclear whether the in-depth density profile observed in our recent study can be explained by such a carbon deposition process within a realm of possibility.

It is the purpose of the present study to analyze the ablation behavior of LATS through a thermal response calculation by accounting for coking. For this purpose, a computer code named super charring materials ablation (SCMA)[3-4)] is updated

to be able to evaluate a material density variation as a result of the deposition of carbon during the diffusion of the pyrolysis gas through the char layer. In the current version of SCMA, the thermal response analysis under a steady-state ablation condition is possible[4] in addition to an unsteady state ablation condition developed originally[3]. In the present study, a coking process is modeled under the assumption of the steady state ablation condition.

There is no information about detailed coking kinetics. In the past study for an Apollo ablator analysis[1], an approximate approach was taken to calculate a carbon deposition process in the char layer. A similar approach will be taken in the present study as a first step toward a detailed modeling for coking.

## 2. Computational Method

Thermal decomposition, heat diffusion, and coking processes within an ablator are calculated in one-dimensional space. A present ablation model is schematically shown in Fig.1. A charring ablator is typically divided into three zones: virgin, pyrolysis, and coking, respectively. Because the details for the processes in thermal decomposition, and thermal diffusion within three zones are given by the same equations in the original SCMA code[3-4], the explanation for these processes is omitted. A model for the solid carbon deposition in the coking zone shown in Figs.1(a), and 1(b) will be explained next in detail.

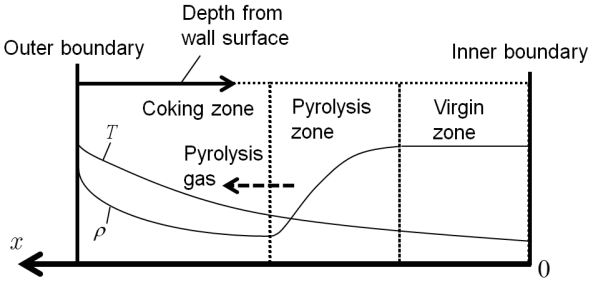


(a) Charring processes within ablator

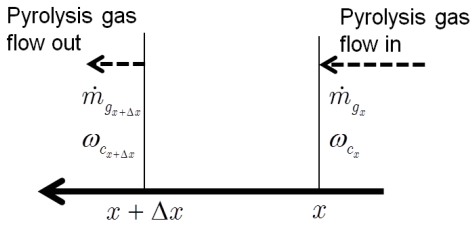


(b) Control volume within coking zone

Fig.1. Schematic diagram of the present ablation model

### 2.1. Coking equation[1]

When solid carbon is deposited within a control volume of the char zone (see Fig.1(b)), the consumption rate of carbon in a pyrolysis gas within the control volume can be written

$$\frac{\omega_{c_{x+\Delta x}}\dot{m}_{g_{x+\Delta x}}-\omega_{c_x}\dot{m}_{g_x}}{\Delta x} \tag{1}$$

When the residence time of the pyrolysis gas within the ablator is ignored, the derivative of mass flux nearly equals the consumption rate of carbon as follows:

$$\frac{\partial \dot{m}_{g_x}}{\partial x}=\frac{1}{\Delta x}\left(\omega_{c_{x+\Delta x}}\dot{m}_{g_{x+\Delta x}}-\omega_{c_x}\dot{m}_{g_x}\right) \tag{2}$$

The first term in the parenthesis of the right hand side of Eq. (2) is transformed into

$$\omega_{c_{x+\Delta x}}\dot{m}_{g_{x+\Delta x}}=\left(\omega_{c_x}+\frac{\partial\omega_{c_x}}{\partial x}\Delta x\right)\left(\dot{m}_{g_x}+\frac{\partial\dot{m}_{g_x}}{\partial x}\Delta x\right) \tag{3}$$

Putting Eq.(3) into the right hand side of Eq.(2), we have the following relation for first-order accuracy in space:

$$\begin{aligned}&\frac{\omega_{c_{x+\Delta x}}\dot{m}_{g_{x+\Delta x}}-\omega_{c_x}\dot{m}_{g_x}}{\Delta x}\\&=\frac{\left(\omega_{c_x}+\frac{\partial\omega_{c_x}}{\partial x}\Delta x\right)\left(\dot{m}_{g_x}+\frac{\partial\dot{m}_{g_x}}{\partial x}\Delta x\right)-\omega_{c_x}\dot{m}_{g_x}}{\Delta x}\\&\approx\dot{m}_{g_x}\frac{\partial\omega_{c_x}}{\partial x}+\omega_{c_x}\frac{\partial\dot{m}_{g_x}}{\partial x}\end{aligned} \tag{4}$$

Using the last equation in Eq. (4), Eq.(2) can be rearranged to:

$$\frac{\partial\dot{m}_{g_x}}{\partial x}=\frac{\dot{m}_{g_x}}{\left(1-\omega_{c_x}\right)}\frac{\partial\omega_{c_x}}{\partial x} \tag{5}$$

By accounting for the conservation of mass of carbon, the production rate of coked solid carbon is given by

$$\frac{\partial\rho_{coke}}{\partial t}=R_{coke}=-\frac{\dot{m}_{g_x}}{\left(1-\omega_{c_x}\right)}\frac{\partial\omega_{c_x}}{\partial x} \tag{6}$$

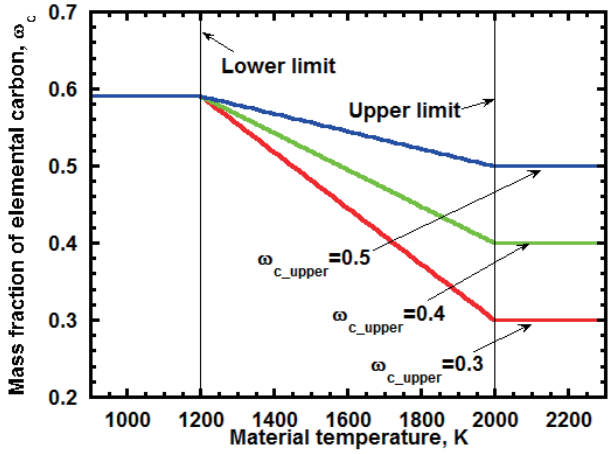


Fig.2. Variation of mass fraction of elemental carbon in a pyrolysis gas for coking

A mass fraction for the elemental carbon in a pyrolysis gas is needed in order to calculate the coking equation given by Eq.(6). In the past study[1], the carbon mass fraction is assumed to be given by a function of temperature and pressure. Because the dependency of the carbon mass fraction on thermophysical and thermochemical state in the char layer is not known for the low density ablator analyzed in the present study, its temperature dependence is modeled in a similar way to the past one: its pressure dependence is uncertain because measured material density variation is confirmed only for one arcjet operating condition[2]; thus the pressure dependence is ignored. As is shown in Fig.2, the mass fraction value is given by assuming that it is linearly decreased under a certain range

of temperature. The initial temperature at which coking begins is taken to be 1200K. Coking is assumed to end until 2000K. The temperature range is nearly the same one in the past model[1]. Three different values for the effective mass fraction of the elemental carbon at the upper temperature, $\omega_{c\_upper}$, are tested, as shown in Fig.2.

### 2.2. Governing equations

Conservation equations for resin, deposited carbon and total energy are given by:

$$\frac{\partial \rho_r}{\partial t} = -R_{pyro} \tag{7}$$

$$\frac{\partial \rho_{coke}}{\partial t} = R_{coke} \tag{8}$$

$$\begin{aligned}(\rho_c c_{p_c} + \rho_r c_{p_r})\frac{\partial T}{\partial t} &= \frac{\partial}{\partial x}\left(\kappa \frac{\partial T}{\partial x}\right) \\ -\dot{m}_g c_{p_g}\frac{\partial T}{\partial x} &+ \left(h_g - h_r\right)\frac{\partial \rho_r}{\partial t} + \left(h_g - h_c\right)\frac{\partial \rho_{coke}}{\partial t}\end{aligned} \tag{9}$$

$$\frac{\partial \dot{m}_g}{\partial x} = R_{pyro} - R_{coke} \tag{10}$$

Total solid mass density is given by

$$\rho_s(x,t) = \rho_r(x,t) + \rho_{coke}(x,t) + \rho_c \tag{11}$$

In the above equations, it is assumed that the decomposition process of resin and the deposition of carbon occur independently. This assumption is likely to be valid because the two processes are developed at different temperature ranges. In order to solve Eqs. (7) to (9) simultaneously, the SCMA code[3-4] is used by retaining as many of the elements in the code. The boundary condition at the heating surface is approximately given by only accounting for the pyrolysis gas injection in the blowing correction term via the Potts formula[5].

### 2.3. Material thermophysical parameters and pyrolysis gas properties

Because the thermophysical properties of LATS are presently unknown, most of the properties needed to solve Eqs. (7)-(9) are taken from available literatures[3,4,6-8] except for the enthalpy and chemical composition of a pyrolysis gas, and thermal conductivity of material. The details will be explained next.

The pyrolysis gas is assumed to consist of C, CH, $CH_2$, $CH_3$, $CH_4$, CO, $CO_2$, $C_2$, $C_3$, H, $H_2$, HO, $H_2O$, O, and $O_2$. The initial elemental composition of the pyrolysis gas is taken as C:H:O=0.591:0.119:0.29 by mass. This ratio is taken from a past study[8], in which the decomposition kinetics of phenolic resin were examined in detail. When the mass fraction of carbon is decreased due to coking, the mass ratio for H and O is calculated by keeping the initial ratio between H and O unchanged. By taking the pyrolysis gas pressure within the material to be constant, the enthalpy of the pyrolysis gas is calculated with a given set of temperature and pressure. A look-up table of enthalpy and chemical equilibrium compositions has been prepared. These properties are calculated using a free energy minimization technique[9,10] as a function of pressure, temperature and mass fraction of carbon over the pressure ranges from $1.0\text{x}10^{-4}$ to 1 atm and the temperature ranges from 500 to 3000K, and the ranges for the mass fraction of carbon from 0.2 to 0.6, respectively. It should be noted that the pressure value of pyrolysis gas within a porous char is taken to be the same as the pitot pressure value measured in the arcjet testing, as will be explained later.

The thermal conductivity value is given by modifying that of a different low density ablator[7]. The present calculation shows no satisfactory agreement of the in-depth and surface temperatures between measurement and calculation when the original thermal conductivity is used. Because the present study is focused on the thermal response analysis within a char layer, we modify the value of the thermal conductivity to reproduce the time history of the measured temperatures in particular within the char layer during testing. To obtain a satisfactory agreement, we multiply 0.4 to the original thermal conductivity value.

## 3. Experimental

Although the details on the experimental approach have been explained in our recent paper[2], a brief explanation will be made for the purpose of completeness.

A LATS material with the specific gravity of about 0.3 was heated in a 20kW arcjet wind tunnel at Japan Ultra-high Temperature Materials Research Center. Nitrogen is used as a test gas. The cold wall heat transfer rate is measured using a copper calorimeter. The stagnation pressure is measured by a Pitot tube. The heat flux and the pitot pressure values are $2\text{MW/m}^2$ and 0.8kPa, respectively. The mass-averaged enthalpy is estimated to be about 9.2MJ/kg. The testing time for the experiments is 70 seconds. Based on the operational condition in the 20kW arcjet wind tunnel so chosen, we can avoid a possible surface degradation due to oxidation. Thus, little geometrical degradation of the tested specimen is expected for this case. This aspect is important to measure the density distribution.

The heated test specimens are shaved with a file. The thickness of the shaved thin sections is about 1-2mm. The number of the sections is about 10 to 20. Each of the sections is weighted with an electronic precision balance. The density of each section is evaluated assuming that the shaved material is in the form of the cylindrical geometry. The experimental error for this density measurement is estimated to be about 5%.

## 4. Results

### 4.1. Overall feature of computed solution

Calculations are carried out for the case of $p_{st}$=0.8kPa, and $q$=$2\text{MW/m}^2$ by accounting for coking effect. The computed in-depth density and temperature profiles are shown in Figs.3 and 4, respectively. The results are presented to demonstrate how the density within a char layer is evolved when the present coking model is used. In the figures, the result with $\omega_{c\_upper}$=0.4 is shown for the case with coking. In Fig. 3(a), the calculated material density distribution for the case without

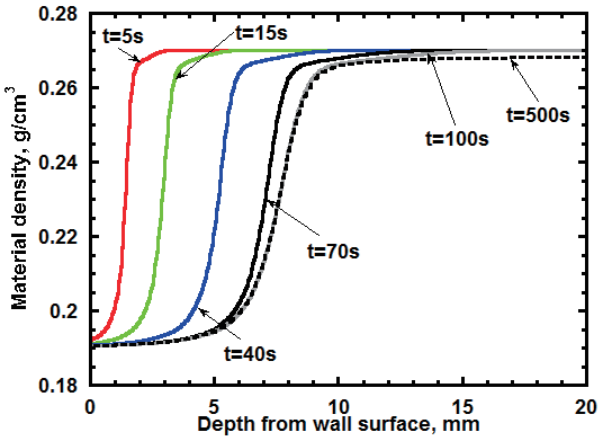


(a) Without coking

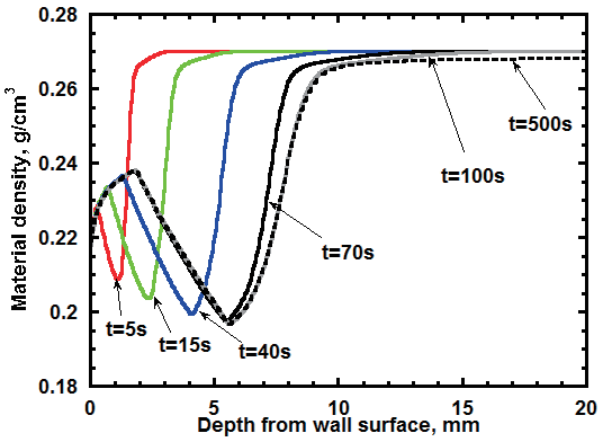


(b) With coking

Fig. 3. Calculated time history of in-depth density distributions.

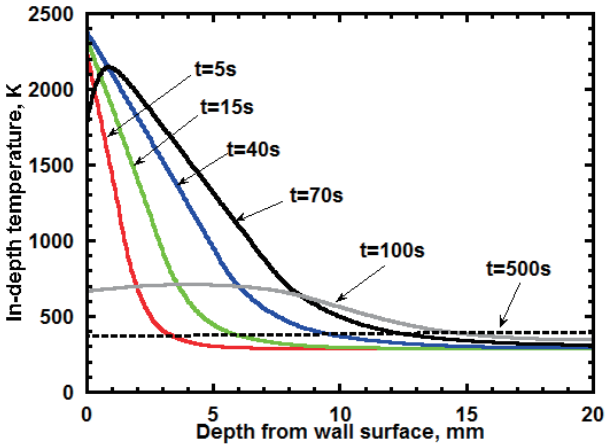


Fig. 4. Calculated time history of the in-depth temperature distribution.

coking is given for comparison, in which $R_{coke}$ is taken to be 0 and the temperature dependence of $\omega_c$ is neglected. It should be noted that the char density without coking is estimated to be 0.19 for this case[2]. Because there is little discernible difference of the calculated temperature distribution between with and without coking, the temperature result without coking is omitted.

One can see from Figs. 3(a), and 3(b) that an interface where a pyrolysis reaction occurs deepens toward the back surface of the ablative material. From Fig. 3(b), in the char layer from the heated surface to the pyrolyzed interface, the density value increases toward the wall surface, while such a trend is not seen in the same zone shown in Fig. 3(a) for the case without coking. In the region where the density increases, the temperature varies from 1200 to 2000K, as shown in Fig. 4. The density value in the char layer increases due to the deposition of solid carbon in the present model. One may find from Fig. 3(b) that the density value decreases from a local peak up to the surface. In the region where coking process ends at an earlier time, which corresponds to the one nearer to the surface, the amount of the carbon deposition is lower as compared with the inner region in the char layer. As a result, the density value decreases in the region very close to the wall surface.

### 4.2. Comparison with experiment

In Figs. 5(a), and 5(b), comparison of the surface and in-depth temperatures during testing until $t$=70s is made, respectively, between calculation and measurement. From the figures, a satisfactory agreement of the surface and the in-depth temperatures at 5 and 10mm is seen between measurement and calculation. It should be noted that this agreement is due to the fact that the thermal conductivity is modified, as explained earlier. The cooling behavior of the ablative material after testing time is not reproduced by the present calculation. In addition, calculation underestimates the time history of the in-depth temperature at the position of 15mm from the surface during all testing time. Thus, the in-depth temperature is predicted by using the present method only over the char layer within the material during heating.

The calculated in-depth density profiles are compared with the experimental data in Fig.6. Calculated results are given at a nearly converged state of $t$=450s. The results are shown for the cases with $\omega_{c\_upper}$= 0.3, 0.4, and 0.5, respectively. The result for the case without coking is also shown in the figure for reference. The experimental data indicates that the char layer density varies from about 0.19 to about 0.23 g/cm$^3$ near the wall surface within about 5mm from the surface, showing a small plateau in the distribution. The calculation without coking underestimates the measured profile near the surface. By accounting for coking, calculated in-depth density profile near the surface approaches the measured one. A moderate difference in the in-depth density profile is seen among the $\omega_{c\_upper}$ values chosen. As shown, a reasonable agreement of the char layer density is obtained when the $\omega_{c\_upper}$ value is taken to be 0.4.

### 4.3. Comparison of calculated data between with and without coking

For the same heating condition calculated in the previous section, calculated data are compared between with and without coking effect. The result with $\omega_{c\_upper}$=0.4 is presented for the case of coking. The calculated pyrolysis gas flow rates ejected out from the material surface are plotted against the elapsed time in Fig. 7. Because coking is accounted for, the

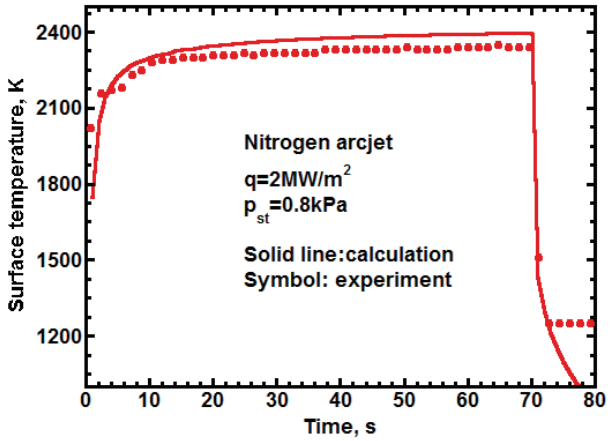


(a) Surface temperature

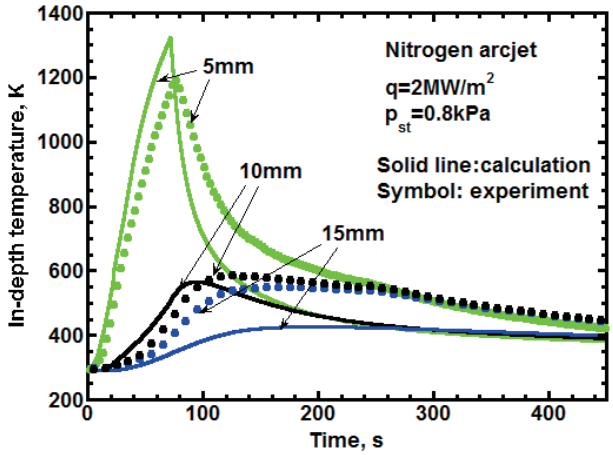


(b) In-depth temperatures

Fig. 5. Comparison of temporal variation of surface and in-depth temperatures between calculation and measurement.

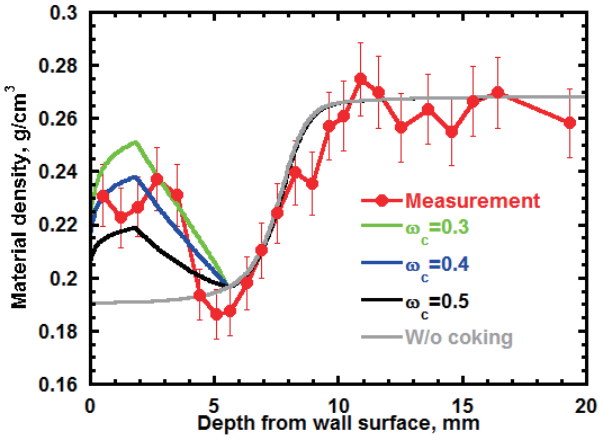


Fig. 6. Comparison of the post-test in-depth density distribution between calculation and measurement.

mass flow rate is decreased toward the wall surface due to the depletion of carbon content in the pyrolysis gas. As a result the ejection rate at the surface is lower as compared with the one without coking.

In Fig. 8, the heating and cooling rates at the wall surface

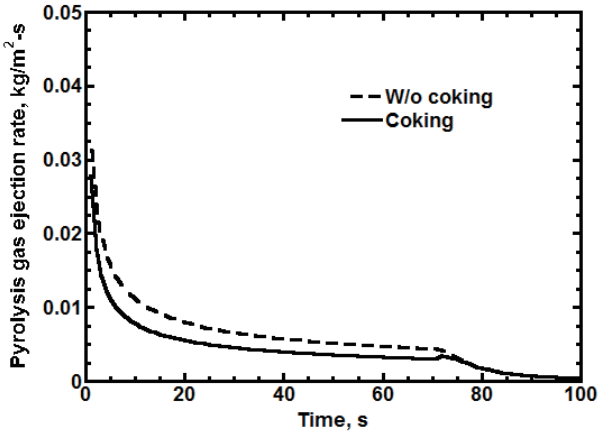


Fig. 7. Comparison of the injection rate of the pyrolysis gas at the outer boundary of the test specimen between with and without coking effect.

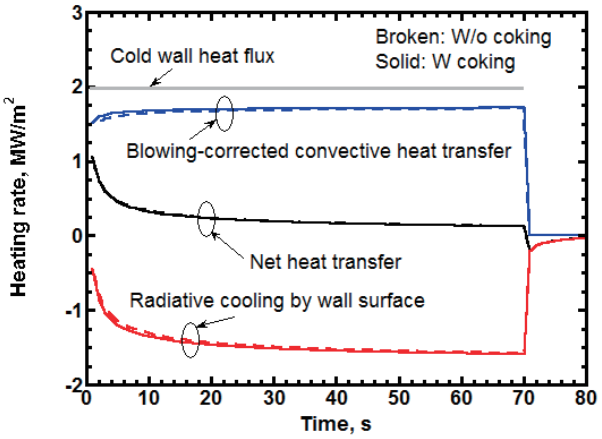


Fig. 8. Comparison of the heating rate at the outer boundary of the test specimen between with and without coking effect.

are plotted against the elapsed time. A net heating rate is given by the sum of the two terms: a blowing-corrected convective heat transfer and a radiative cooling. Due to the reduction of the mass ejection rate, the calculated convective heat transfer rate with coking is higher than the one without coking, but the difference between the two cases is only slight. The surface temperature is increased only slightly by following the trend in the convective heat transfer with coking. As a result, little difference of the net heat transfer rate is seen between with and without coking for the case analyzed in the present study.

By using the developed code, the chemical composition of the ejected pyrolysis gas into a boundary layer can be evaluated. In Fig. 9, the mole fractions of the primary chemical species in the ejected pyrolysis gas, $H_2$, H, CO, $C_3$, and $C_2$, are plotted against the elapsed time for the cases with and without coking. Because a relative contribution of elemental carbon in the ejected gas becomes smaller, the mole fraction of the carbon containing species is reduced: from comparison, $C_3$ is reduced by a factor of 10; and $C_2$ is decreased nearly by half. Noted that CO is nearly constant for the case analyzed. The mole fraction of H and $H_2$ is

increased by about 10% compared with the result without coking.

## 5. Discussions

A fair agreement of the in-depth density distribution between measurement and calculation indicates that the increase in the in-depth density near the surface of the ablative material heated in an arcjet wind tunnel could be due to the deposition of solid carbon on the char layer. The present calculation shows that the increase in the measured density profile is reproducible reasonably if the $\omega_c$ value at the upper limit temperature is assumed to be decreased by about 23% as compared with the initial mass fraction of carbon in a pyrolysis gas. The past analysis of a post-test ablative material used in the Apollo missions showed that an $\omega_c$ value could be reduced by about 30% from the initial mass fraction of carbon in a pyrolysis gas over the temperature range from 1250 to 2000K.[1)] It is found that the $\omega_c$ value deduced in the present study ($\omega_c$ varies from 0.591 to 0.400 for the temperature ranges from 1200 to 2000K) shows nearly the same trend obtained in the past study.

It should be noted that the present study cannot fully confirm how coking affects the effectiveness of the convective blockage at an ablating surface. The calculated mass ejection rate for the case with coking reduces typically by about 20 to 30% as compared with the one without coking. This reduction in mass injection rate will reduce the convective blockage effect. In contrast, the calculated molecular weight of the injection gas accounting for coking is 8.8g/mol, which is lower than the value of 11g/mol for the case without coking. A past study showed that the effectiveness of convective blockage could be increased when the molecular weight of injection gas is reduced[11)]. How these two competing mechanisms are balanced is unknown. In order to examine the effect of coking on the convective blockage effect, an integrated approach[12)] may be necessary to calculate an interaction process between an arcjet freestream and an ejected pyrolysis gas. Such a task is left in the future.

In addition, the present calculation suggests that a radiative heating condition in a flight with a high entry velocity may be modified due to coking effect. Because the carbon containing chemical species can absorb the radiation emanating from an inviscid shock layer in the ablation layer, the reduction of $C_3$ due to coking might increase radiative heating if the surface recession is relatively small. Efforts should be made in the future to investigate such an effect of coking on radiative heating.

## 6. Concluding Remarks

By using an upgraded charring material ablation code, in which a carbon deposition process within a char layer is accounted for, it is found that the experimentally obtained in-depth density increase in the char layer of a low density ablative material can be explained by the deposition of about

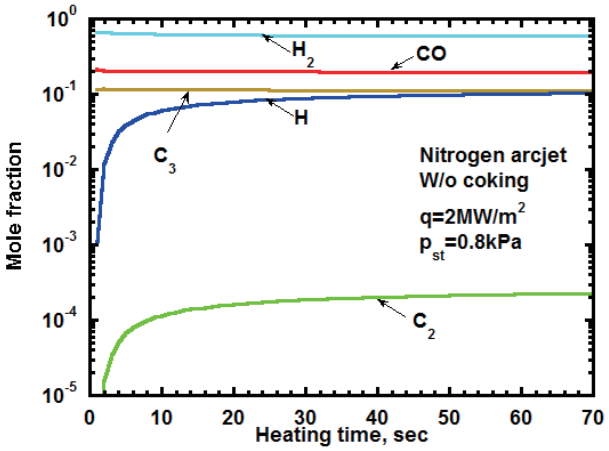


(a) Without coking

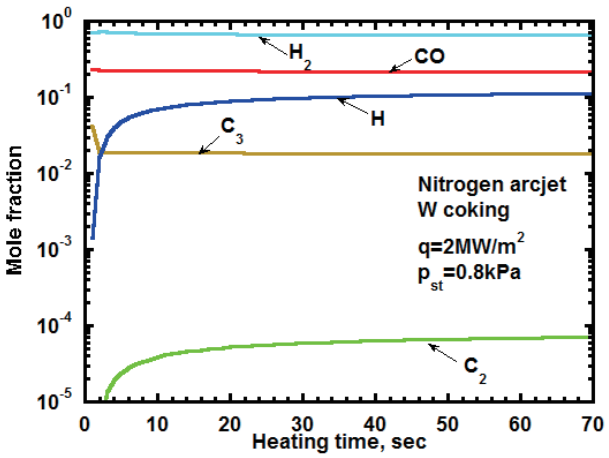


(b) With coking

Fig. 9. Comparison of the mole fraction of the pyrolysis gas at the outer boundary of the test specimen between with and without coking effect.

23% of mass fraction of carbon contained originally in a pyrolysis gas when it diffuses within a porous char layer. The present calculation indicates that carbon deposition could occur within about 5mm thickness from surface in the char layer. These trends are consistent with the results observed in a past study. The present computational approach can be used to predict the chemical composition of pyrolysis gas ejected into the boundary layer over the ablative material. The present method is applicable in the future to a more realistic ablative environment in which surface recession occurs in order to examine the effect of coking on ablation behaviors.

**Acknowledgments**

This research was supported by the Japan Society for Promotion of Science as Grant-in-Aid for Scientific Research, No. 21360423.

### References

1) Bartlett E.P., Abbett, M.J., Nicolet, W. E., and Moyer C. B.: Improved Heat-Shield Design Procedures for Manned Entry Systems, Part II, Application to Apollo, Aerotherm Final Report No. 70-15, 1970.

2) Kobayashi Y., Sakai T., Suzuki T., Fujita K., Okuyama K., Kato S., and Kitagawa K.: An Experimental Study on Thermal Response of Low Density Carbon-Phenolic Ablators, AIAA Paper 2009-1587, January, 2009.
3) Ahn, H.–K., Park, C., and Sawada, K.: Response of Heatshield Material at Stagnation Point oh Pioneer-Venus Probe, *Journal of Thermophysics and Heat Transfer*, Vol. 16, No. 3, 2002, pp. 432-439.
4) Suzuki, T.: Study Of Ablative Heatshield for Entry Capsule, Ph.D Dissertation, Department of Aeronautics and Space Engineering , Tohoku University, 2004
5) Potts, R.L.: Application of Integral Methods to Ablation Charring Erosion, A review, *Journal of Space craft and Rockets*, Vol.32, No.2, 1995, pp.200-209.
6) Suzuki T., Fujita K., Okuyama K., Sakai T., and Kato S., 'Modeling of Thermal decomposition process of a low density ablator with TGA analysis', JAXA Research and Development Report (in Japanese) edited by Fujita K. and Suzuki T..
7) Tran, H., Johnson, C., Rasky, D., Hui, F., Chen, Y.K., Hsu, M., "Phenolic Impregnated Carbon Ablators (PICA) for Discovery Class Missions," AIAA Paper 96-1911, June, 1996
8) Sykes, G. F.: Decomposition Characteristics of A char-Forming Phenolic Polymer Used For Ablative Composites, NASA TN-D 3810, September, 1966.
9) Gordon S., and McBride, B. J.: Computer Program for Calculation of Complex Chemical Equilibrium Compositions, Rocket Performance, Incident and Reflected Shocks and Chapman-Jouguet Detonations," NASA SP-273, February 1971.
10) Perini, L. L.,: Curve Fits of JANAF Thermochemichal Data," The Johns Hopkins University, ANSP-M-5, September, 1972.
11) Mills, A. F. and Wortman, A.: Two- Dimensional Stagnation Point Flows of Binary Mixtures, *Int J. Heat Mass Transfer*, Vol.15, pp.969-987
12) Suzuki, T., Sakai T., and Yamada T.: Calculation of Thermal Response of Ablator Under Arc-Jet Condition,'' *Journal of Thermophysics and Heat Transfer*, Vol.21 No.2, 2007, pp.257-266.